Transfer Matrices and Partition-Function Zeros for Antiferromagnetic Potts Models

II. Extended results for square-lattice chromatic polynomial

Jesper Lykke Jacobsen
Laboratoire de Physique Théorique et Modèles Statistiques
Université Paris-Sud
Bâtiment 100, F-91405 Orsay, FRANCE
JACOBSEN@IPNO.IN2P3.FR

Jesús Salas
Departamento de Física Teórica
Facultad de Ciencias, Universidad de Zaragoza
Zaragoza 50009, SPAIN
JESUS@MELKWEG.UNIZAR.ES

November 27, 2000
Revised February 9, 2001

Abstract

We study the chromatic polynomials for $m \times n$ square-lattice strips, of width $9 \leq m \leq 13$ (with periodic boundary conditions) and arbitrary length n (with free boundary conditions). We have used a transfer matrix approach that allowed us also to extract the limiting curves when $n \to \infty$. In this limit we have also obtained the isolated limiting points for these square-lattice strips and checked some conjectures related to the Beraha numbers.

Key Words: Chromatic polynomial; chromatic root; antiferromagnetic Potts model; square lattice; transfer matrix; Fortuin-Kasteleyn representation; Beraha–Kahane–Weiss theorem; Beraha numbers.

1 Introduction

The antiferromagnetic q-state Potts model [1, 2, 3] has many interesting features. First, for large enough q the model exhibits a nonzero ground-state entropy (without frustration). This is important as it provides an exception to the third law of thermodynamics [4, 5]. Second, the antiferromagnetic Potts model has a rich phase diagram that depends explicitly on the lattice structure (in contrast to the universality typically enjoyed by ferromagnets). It therefore becomes interesting to elucidate which features of the lattice structure (e.g., coordination number, dimensionality, etc) correlate with the critical properties of the model (or the absence of criticality). Furthermore, for each lattice G there is a number $q_c(G)$ such that for all $q > q_c$ the Potts model is disordered at any temperature (including $T = 0$); at $q = q_c(G)$ the system is disordered at all positive temperatures and has a zero-temperature critical point. Third, the study of Potts antiferromagnets is closely related to graph theory. Namely, the zero-temperature limit of the antiferromagnetic Potts model partition function is just the chromatic polynomial $P_G(q)$:

$$\lim_{T \to 0} Z_G(q;T) = P_G(q). \tag{1.1}$$

This quantity equals the number of ways of coloring the vertices of the graph G with q colors, with the constraint that no adjacent vertices have the same color [6]. Finally, there are condensed-matter systems that can be modeled using Potts antiferromagnets. In particular, the insulator $SrCr_{8-x}Ga_{4-x}O_{19}$ can be described using a three-state Kagomé-lattice Potts antiferromagnet [7, 8].

One interesting question is the value of the number $q_c(G)$ for the most common regular lattices G. There are general analytic bounds in terms of the coordination number Δ of the lattice (e.g., $q_c \le 2\Delta$ [9]), but they are not very sharp. An alternative approach, inspired by the Lee–Yang picture of phase transitions [10], is to study the zeros of the chromatic polynomial when the parameter q is allowed to take complex values (see Ref. [11] for a complete list of references). The best results concern families G_n of graphs for which the chromatic polynomial can be expressed via a transfer matrix of fixed size $M \times M$:

$$P_{G_n}(q) = \mathrm{tr}[A(q)\, T(q)^n] \tag{1.2a}$$

$$= \sum_{k=1}^{M} \alpha_k(q)\, \lambda_k(q)^n, \tag{1.2b}$$

where the transfer matrix $T(q)$ and the boundary-condition matrix $A(q)$ are polynomials in q, so that the eigenvalues $\{\lambda_k\}$ of T and the amplitudes $\{\alpha_k\}$ are algebraic functions of q.

The two best understood cases of the Potts antiferromagnet are the square and triangular lattices. In this paper we consider the square lattice. For $q = 2$ this model undergoes a finite-temperature second-order phase transition. For $q = 3$ there is strong analytic and numerical support for a zero-temperature critical point [12, 13, 14, 15, 16, 17, 18, 19], though a rigorous proof is (to our knowledge) still lacking.

For $q = 4$ Monte Carlo simulations show that the model is disordered even at zero temperature [19]. It thus seems clear that $q_c(\mathrm{sq}) = 3$.

In the transfer matrix approach, the goal is to compute the transfer matrix T for a square-lattice strip of width m with some boundary conditions. With this matrix one can easily compute the chromatic-polynomial zeros of any finite strip $m \times n$. In addition, one can also compute the accumulation points when $n \to \infty$. According to the Beraha–Kahane–Weiss theorem [20, 21], the zeros when $n \to \infty$ can either be isolated limiting points (when the amplitude associated to the dominant eigenvalue vanishes) or form a limiting curve $\mathcal{B}$ (when two dominant eigenvalues cross in modulus). By studying the limiting curves for different values of the width m we hope to learn new features of the thermodynamic limit $m \to \infty$.

The first results for the square lattice using this approach were obtained by Shrock and collaborators.[1] They studied strips up to $m = 6$ (resp. $m = 5$) with cylindrical (resp. free) boundary conditions[2] [22, 23, 24]. They also computed square-lattice strips with cyclic and toroidal boundary conditions up to $m = 4$ [24, 25, 26, 27, 28, 29, 30]. The results with free and cylindrical boundary conditions were extended to $m \leq 8$ in Ref. [11]. The qualitative shape of the limiting curve found for these boundary conditions is quite similar to the one found by Baxter in case of the triangular lattice [31], but with the zero-temperature critical point lying at $q_c(\mathrm{sq}) = 3$ rather than at $q_c(\mathrm{tri}) = 4$.

However, there may be an important qualitative difference between the triangular-lattice and square-lattice cases, concerning the number of times that the infinite-volume curve $\mathcal{B}$ crosses the positive real q-axis. In physical terms this corresponds to the number of intervals of the real q-axis where the ground-state entropy $S_0(q)$ has a distinct analytic form, or in other words to the number of "phases" that the model has as q is varied [25, 32]. For many (but not all) finite strip widths m, we find that the limiting curve $\mathcal{B}$ crosses the real axis at a point $q_0(m)$.[3] It is reasonable to expect that there are infinitely many such widths m and that $q_0(m)$ tends to a limiting value $q_0(\infty)$ as $m \to \infty$. One could be tempted to assume that $q_0(\infty) = q_c$; but this, it turns out, is not always true. Indeed, in the triangular-lattice case, Baxter's exact solution [31] shows that $q_0(\mathrm{tri}) \approx 3.81967$ while $q_c(\mathrm{tri}) = 4$; this is because the infinite-volume curve $\mathcal{B}$ crosses the real q-axis *twice* in the interval $0 < q < \infty$. Thus, in general one cannot identify q_0 with q_c.[4] On the other hand, our data for the square

[1] They actually used a generating-function approach which is equivalent to transfer matrices.

[2] Let m (resp. n) denote the number of sites in the transverse (resp. longitudinal) direction of the strip, and let F (resp. P) denote free (resp. periodic) boundary conditions in a given direction. Then we use the terminology: free ($m_\mathrm{F} \times n_\mathrm{F}$), cylindrical ($m_\mathrm{P} \times n_\mathrm{F}$), cyclic ($m_\mathrm{F} \times n_\mathrm{P}$), and toroidal ($m_\mathrm{P} \times n_\mathrm{P}$).

[3] For those lattice strips where q_0 cannot be strictly defined because $\mathcal{B}$ does not cross the real axis, the limiting curve often includes a pair of complex-conjugate endpoints that are very close to the positive real q-axis. In these cases, we define q_0 to be the endpoint closest to that axis with positive imaginary part.

[4] One can qualitatively think of q_c as the limit of the (complex) rightmost endpoints of the limiting curve $\mathcal{B}$ as the lattice strip width m increases. These endpoints can be defined in most cases

lattice suggest that $q_0(\infty)$ may well be equal to $q_c = 3$. If this is true, the qualitative shape of the infinite-volume curve $\mathcal{B}$ for the square lattice will be rather different from that found for the triangular lattice. In particular, region $\mathcal{D}_2$ in Figure 5 of ref. [31] will be "narrowed" along the q-axis so the points F (i.e., q_0) and C (i.e., q_c) coincide. Thus, region $\mathcal{D}_2$ will be split into two complex-conjugate regions that may or may not intersect the positive real q-axis at q_c.

In this paper we extend the results of [11] by computing the transfer matrices for square-lattice strips of width $9 \le m \le 13$ with periodic boundary conditions in the transverse direction and free boundary conditions in the longitudinal direction. We have chosen this type of boundary conditions because we expect it to provide a faster approach towards the thermodynamic limit than we would have obtained using free boundary conditions in both directions, while at the same time avoiding the technical complications implied by the imposition of doubly periodic (toroidal) boundary conditions [35]. The present computation has been possible thanks to a more efficient algorithm than the one employed in [11]; this improved algorithm allows us to handle transfer matrices as large as 498×498. The transfer matrices, of course, enable us to compute the chromatic polynomials $P_{m\times n}(q)$ for any finite length n. For $9 \le m \le 11$, however, we have been able to obtain the limiting curves $\mathcal{B}$ directly in the limit $n \to \infty$, by using the same methods as in [11]. When possible, we have also computed the isolated limiting zeros for these square-lattice strips and checked whether the conjectures put forth in [11, Section 7] hold true. These conjectures are related to the Beraha numbers [36] which seem to play a special role in the theory of chromatic polynomials (see Ref. [11] and references therein):

$$B_n = 4\cos^2\frac{\pi}{n} = 2 + 2\cos\frac{2\pi}{n}, \quad \text{for } n = 2, 3, \ldots . \tag{1.3}$$

We find that the limiting curves $\mathcal{B}$ for various system sizes are qualitatively quite similar; however, they show noticeable differences depending on whether the width m is even or odd. In particular, we conjecture that only the limiting curves for odd m cross the real axis, thus giving a well-defined value of q_0. Our best estimate for this quantity (assuming monotonicity with the strip width) reads

$$q_0(\mathrm{sq}) \gtrsim 2.9161885031 \tag{1.4}$$

This estimate is quite close to the expected value for $q_c(\mathrm{sq}) = 3$. For the square-lattice strips with even width m we find for $m \ge 8$ that there is a small gap separating $\mathcal{B}$ from the real axis: the real part of the points closest to that axis is slightly smaller than the value of q_0 for widths $m \pm 1$, and based on our numerical data we conjecture that the imaginary part of such points goes to zero as $B_5^{-m/2}$.

We finally conjecture (based on our numerical evidence) that $q_0(\mathrm{sq}) = q_c(\mathrm{sq}) = 3$. This equality has important implications on the analytic structure of the free energy

for free boundary conditions in the longitudinal direction [11, 33], but not for periodic boundary conditions in the longitudinal direction [34]. When m grows large, those endpoints approach the real q-axis, and in the limit $m = \infty$ they pinch that axis at $q = q_c$.

in the thermodynamic limit. In the zero-temperature triangular-lattice Potts antiferromagnet, we have that $q_0(\mathrm{tri}) \neq q_c(\mathrm{tri})$ and there are three domains of analyticity of the free energy [31]. Furthermore, all these three domains intersect the real q-axis; q_0 and q_c are the boundaries of such domains on the positive real q-axis. In the zero-temperature square-lattice Potts antiferromagnet, we have that $q_0(\mathrm{sq}) = q_c(\mathrm{sq})$. Thus, on the real q-axis there are only two domains of definition whose boundary is precisely q_c. This is a valuable piece of information about the analytic structure of the free energy of this model whose solution is yet to be found.

This paper is laid out as follows: In Section 2 we explain the method used to compute the transfer matrices. The necessary background can be found in [11]. In Section 3 we expose our numerical results for square-lattice strips with cylindrical boundary conditions. Finally, Section 4 is dedicated to our conclusions.

2 Transfer Matrix Algorithm

The general theory of Potts model transfer matrices has been reviewed in [11, Section 3], and in what follows we shall therefore limit ourselves to a rather concise and more informal description. The main emphasis is on the algorithmic improvements over Ref. [11], which have enabled us to extend the computations to strips of width $9 \leq m \leq 13$ with cylindrical boundary conditions.

Let $G = (V, E)$ be a finite undirected graph with vertex set V and edge set E, and let $\{J_e\}_{e \in E}$ be a set of coupling constants. In the Fortuin-Kasteleyn representation [37, 38] the partition function of the q-state Potts model defined on G reads

$$Z_G(q, \{v_e\}) = \sum_{E' \subseteq E} q^{k(E')} \prod_{e \in E'} v_e, \tag{2.1}$$

where $k(E')$ is the number of connected components (clusters) in the subgraph (V, E'), and $v_e = \exp(\beta J_e) - 1$. The main advantage of this representation is that q can now be analytically continued to complex values. However, the price to be paid is that the Boltzmann weights contain the non-local factor $q^{k(E')}$.

Although this non-locality would seem to inhibit the construction of the transfer matrix, the problem can be circumvented by working in a basis of connectivities $\mathcal{C}_m$, containing information about how the m spins in a given time slice t are interconnected in the portion of (V, E') that is prior to t. Clearly, the number $C_m = |\mathcal{C}_m|$ of such connectivities is equal to the number of ways that m points on the rim of a disc can be connected in the interior of the disc, by means of a planar graph. The evaluation of these numbers is a standard combinatorial exercise [39], and one arrives at the Catalan numbers,

$$C_m = \frac{(2m)!}{m!(m+1)!}. \tag{2.2}$$

A numerical implementation of the Potts model transfer matrix in the basis of Catalan connectivities was first described by Blöte and Nightingale [40]. These authors also introduced a *ranking* of the connectivities, i.e. an injective mapping from

$\mathcal{C}_m$ to the set of integers $\{1, 2, \ldots, C_m\}$. Details on the construction of the inverse mapping were given in [41]. The idea is then to use the integers to index the entries of the transfer matrix, and the connectivities to work out the possible transitions between states along with their respective Boltzmann weights. When combined with a standard sparse matrix factorization, in which the entire transfer matrix is written as a product of elementary matrices each adding one edge of G, this algorithm is highly efficient, since each non-zero matrix element can be computed in time $\sim m$.

Since we are considering specifically the zero-temperature antiferromagnet ($v_e = -1$ for all edges $e \in E$) the dimension of the transfer matrix is actually much less than C_m, since among the m points in a given time slice no pair of neighboring points can belong to the same cluster. It can be shown [11, Section 3.3] that the number $R_m = |\mathcal{R}_m|$ of antiferromagnetically allowed states $\mathcal{R}_m$ is given by the Riordan numbers, $R_0 = 1$, $R_1 = 0$ and

$$R_m = \sum_{k=0}^{m-1} (-1)^{m-k-1} \sum_{j=0}^{\lfloor k/2 \rfloor} \binom{k}{2j} C_j \quad \text{for } m \geq 2. \tag{2.3}$$

Furthermore, due to isotropy and the periodic boundary conditions, the connectivities $\mathcal{R}_m$ are invariant under the action of the dihedral group D_m on the cyclically ordered set of m points in the time slice considered. The appropriate basis states $\mathcal{S}_m$ are thus found from the Riordan states $\mathcal{R}_m$ by symmetrizing with respect to the elements of D_m. The resulting dimension of the transfer matrix SqCyl(m) $= |\mathcal{S}_m|$ has been evaluated in [11, Table 2].

However, the sparse matrix decomposition does not respect any of these constraints, and accordingly the number of connectivities in the intermediary states between to subsequent time slices will still be C_m. To compute a given column $T(q)|s_\mathrm{i}\rangle$ of the transfer matrix, with $|s_\mathrm{i}\rangle \in \mathcal{S}_m$, we therefore proceed as follows. First, each of the distinct states in the set $\{D_m^{(j)}|s_\mathrm{i}\rangle : j = 1, 2, \ldots, 2m\} \subseteq \{C_m\}$ is assigned a weight $q^{k(|s_\mathrm{i}\rangle)}$, where $k(|s_\mathrm{i}\rangle)$ is the number of connected components in $|s_\mathrm{i}\rangle$. Second, we act on this initial state with $T(q)$, or rather with its sparse matrix decomposition. The final state obtained in this manner should again be symmetric with respect to all $D_m^{(j)}$, and it provides a non-trivial check of our algorithm that this is actually the case. Reading now off the weight of each state $\langle s_\mathrm{f}| \in \mathcal{S}_m$, and multiplying by $q^{-k(\langle s_\mathrm{f}|)}$, we deduce the value of the matrix element $\langle s_\mathrm{f}|T(q)|s_\mathrm{i}\rangle$.

A few practical remarks are in order. Since all weights are polynomials in q the computations are done using symbolic algebra, representing the integer coefficients of each power of q in an array. These integers may in principle be very large, and thus cause overflow in a standard 32 bit integer arithmetic. This problem can be easily remedied by using modular arithmetic, i.e. computing all coefficients modulo different primes, and retrieving the complete result from the Chinese remainder theorem. However, for the system sizes used in this work it turned out that 32 bits are actually sufficient.

As usually with transfer matrix methods, the main obstacle for going to large system sizes is due to memory limitations. Our algorithm for $m = 13$ used some 500 MBytes of memory, and although one might have gone to slightly larger systems on

a bigger computer, we refrained from doing so because of the restrictions imposed by the subsequent analysis (see Section 3). The efficiency of our algorithms can be appreciated by noting that the calculations for $m = 8$, the largest system size treated in [11], were done in less than ten seconds. In fact we have reproduced all results given in Ref. [11] for the transfer matrices and the boundary condition vectors (see below) with $m \le 8$; besides validating Ref. [11], this is of course also a nontrivial check on the correctness of our programs.

Apart from the transfer matrix we are also interested in computing the zero-temperature partition functions (i.e., the chromatic polynomials) $P(m_{\rm P} \times n_{\rm F})$ for strips of a finite length n and with free boundary conditions in the longitudinal direction. As explained in [11, Section 6] this can be achieved by sandwiching powers of $T(q)$ between suitable initial and final vectors,

$$P(m_{\rm P} \times n_{\rm F}) = \langle v_{\rm f}|T(q)^{n-1}|v_{\rm i}\rangle. \tag{2.4}$$

The initial vector $|v_{\rm i}\rangle$ is simply the unit vector defined by assigning a weight one to the unique state in which each of the m points belongs to a distinct cluster, and zero to all other states. The final vector $\langle v_{\rm f}|$ corresponds to adding the last row of the lattice, followed by a trace over the final states $\langle s_{\rm f}|$ in which each state is weighted by $q^{k(\langle s_{\rm f}|)}$. It is found by a procedure very similar to the one used to compute the matrix elements $\langle s_{\rm f}|T(q)|s_{\rm i}\rangle$. The only difference is that, in the last step, we take the trace over the $\langle s_{\rm f}|$, rather than projecting on each of them and multiplying by $q^{-k(\langle s_{\rm f}|)}$.

3 Numerical Results for the Square-Lattice Chromatic Polynomial: Periodic Transverse Boundary Conditions

We have computed the transfer matrix $T(q)$ and the limiting curves $\mathcal{B}$ for square-lattice strips of widths $9 \le L_x \le 13$ with periodic boundary conditions in the transverse direction. One direct check of our results is provided by the (trivial) identity

$$Z(m_{\rm P} \times n_{\rm F}) = Z(n_{\rm F} \times m_{\rm P}) \tag{3.1}$$

The chromatic polynomials $Z(n_{\rm F} \times m_{\rm P})$ with $n = 2, 3$ are well-known [42, 29]. We have used both the resultant and the direct-search methods to obtain the limiting curves (see [11] for details). To compute the isolated limiting points we define the matrix $D(q)$:

$$D(q) \;=\; \begin{pmatrix} P_{n\times 1} & P_{n\times 2} & \cdots & P_{n\times M} \\ P_{n\times 2} & P_{n\times 3} & \cdots & P_{n\times M+1} \\ \vdots & \vdots & & \vdots \\ P_{n\times M} & P_{n\times M+1} & \cdots & P_{n\times 2M-1} \end{pmatrix}, \tag{3.2}$$

where M is the dimension of the corresponding transfer matrix. Then it can be proved [43] that

$$\det D(q) = \prod_{k=1}^{M} \alpha_k \prod_{1 \le i < j \le M} (\lambda_j - \lambda_i)^2. \tag{3.3}$$

Thus, all the zeros of the amplitudes α_k are also zeros of $\det D(q)$ (see also [11, Section 2.2]).

3.1 $L_x = 9_{\mathrm{P}}$

The transfer matrix is 22-dimensional; it can be found in the MATHEMATICA file `transfer2.m` that is available with the electronic version of this paper in the `cond-mat` archive at `http://www.lanl.gov`. We have checked that none of the amplitudes vanishes identically.

We have computed the limiting curve $\mathcal{B}$ using the direct-search method. In addition, we were able to compute the resultant at $\theta = 0$ (but unfortunately not for all θ). Some of its zeros are precisely the endpoints of the limiting curve, which is why our results for the endpoints are more accurate in this section than in the following ones.[5] The limiting curve contains nine disconnected pieces (see Figure 1). One of them crosses the real axis at $q \approx 2.8505722621$. There are 20 endpoints:

$$q \approx -0.44699181 \pm 1.24252295\, i \tag{3.4a}$$

$$q \approx 1.14912991 \pm 2.61264326\, i\,; \quad q \approx 1.15312070 \pm 2.61981372\, i \tag{3.4b}$$

$$q \approx 2.36507014 \pm 2.08719033\, i\,; \quad q \approx 2.38763742 \pm 2.08307229\, i \tag{3.4c}$$

$$q \approx 2.83939211 \pm 1.19488272\, i\,; \quad q \approx 2.83111413 \pm 1.16708976\, i \tag{3.4d}$$

$$q \approx 2.84682005 \pm 0.40527862\, i\,; \quad q \approx 2.85144522 \pm 0.40515929\, i \tag{3.4e}$$

$$q \approx 3.01123194 \pm 1.04259193\, i \tag{3.4f}$$

There are eight small gaps defined by the endpoints given in Eqs. (3.4b–3.4e). Finally, there are two T-points at $q \approx 2.854 \pm 1.123\, i$.

We have also computed the polynomial $\det D(q)$ for this strip. It can be written as

$$\begin{aligned} \det D(q) \;=\; & q^{22}(q-1)^{52}(q-2)^{22}(q^2-3q+1)^{19}(q-3)^{42}(q^3-5q^2+6q-1)^7 \\ & (q^2-4q+2)^4(q^3-6q^2+9q-1)(q^2-5q+5)P(q)^2, \end{aligned} \tag{3.5}$$

where $P(q)$ is a polynomial of degree 1170 with integer coefficients (and not factorizable over the integers). The full expression of (3.5) is included in the MATHEMATICA file `transfer2.m`. The pre-factors appearing in (3.5) correspond to the first nine minimal polynomials $p_n(q)$ given in [11, Table 1]. In particular, this

[5] The zeros of the resultant at $\theta = 0$ correspond to values of q such that there are two (or more) equal eigenvalues. However, we are only interested in the values of q associated to *dominant* equal eigenvalues.

means that $\det D(q) = 0$ for the first nine Beraha numbers $B_2, \ldots, B_{10}$, in agreement with Conjecture 7.1 of [11]. Indeed, the first three Beraha numbers $0, 1, 2$ are trivial zeros as all the amplitudes vanish at those values. Thus, they are isolated limiting points. The non-trivial isolated limiting points are the Beraha number $B_5 = (3+\sqrt{5})/2$, and the complex conjugate pairs $q \approx 1.3290624037 \pm 2.5498775371\,i$ and $q \approx 2.5285781385 \pm 1.5750286926\,i$ (see Figure 1).

The convergence to the non-trivial real zero B_5 is quite fast (actually, exponential) as shown in Table 1. The largest real zero in Table 1 converges at an approximate $1/n$ rate to the value $q_0 \approx 2.8505722621$.

We have also checked Conjectures 7.2 and 7.3 of [11], namely that $\det D(q) > 0$ for all $q = B_k$ with $k > 10$. In particular, we have checked this result up to $k = 50$. We expect that the same result holds also for $k > 50$ as $f(k) = \det D(q = B_k)$ is clearly a increasing monotonic function of k.

3.2 $L_x = 10_{\mathrm{P}}$

The transfer matrix is 51-dimensional; it can be found in the MATHEMATICA file `transfer2.m`. We have checked that none of the amplitudes vanishes identically. Unfortunately we were unable to compute the resultant even at $\theta = 0$, so we used a pure direct-search method.

The limiting curve $\mathcal{B}$ contains ten connected pieces. None of them crosses the real axis. The points closest to that axis are $q \approx 2.82813 \pm 0.00097\,i$. We find the following 22 approximate endpoints:

$$q \approx -0.48079 \pm 1.13785\,i \tag{3.6a}$$

$$q \approx 0.94694 \pm 2.61250\,i\,; \quad q \approx 0.94561 \pm 2.60984\,i \tag{3.6b}$$

$$q \approx 2.18917 \pm 2.26882\,i\,; \quad q \approx 2.19871 \pm 2.26845\,i \tag{3.6c}$$

$$q \approx 2.76451 \pm 1.49846\,i\,; \quad q \approx 2.77167 \pm 1.48200\,i \tag{3.6d}$$

$$q \approx 2.82813 \pm 0.00097\,i \tag{3.6e}$$

$$q \approx 2.86581 \pm 0.87778\,i\,; \quad q \approx 2.87243 \pm 0.87284\,i \tag{3.6f}$$

$$q \approx 3.21691 \pm 0.52738\,i \tag{3.6g}$$

There are nine small gaps defined by the endpoints (3.6b–3.6f). Finally, there is a T-point close to $q \approx 2.874 \pm 0.941\,i$.

In this case we have been unable to obtain the polynomial $\det D(q)$ due to lack of computer memory. By inspection of Figure 2 we expect four real limiting points at the first four Behara numbers $q = 0, 1, 2, B_5$. The first two limiting points (i.e., $q = 0, 1$) are trivial ones, as all the amplitudes vanish. We have computed the amplitudes α_k corresponding to $q = 2, B_5$ and, in both cases, the dominant amplitude $\alpha_\star$ vanishes. The convergence to the non-trivial real zeros $q = 2, B_5$ is quite fast as shown in Table 1. There are also three pairs of complex conjugate isolated limiting points: $q \approx 2.7535938496 \pm 0.9533568270\,i$, $q \approx 2.3640435205 \pm 1.8567782883\,i$, and $q \approx 1.0488718011 \pm 2.5727097899\,i$. We have computed the amplitudes corresponding to these values of q. The dominant amplitude is very small for the first two pairs (the

absolute value of that amplitude is respectively $\approx 4.09 \times 10^{-32}$, and $\approx 6.4 \times 10^{-42}$). The dominant amplitude for the last pair is not that small ($|\alpha_\star| \approx 3.03 \times 10^{-4}$). We believe there is an isolated limiting point nearby, but we cannot guess a better estimate as the convergence is still dominated by the $1/n$ ratio coming from the regular points of $\mathcal{B}$. This phenomenon also occurs for $L_x = 9_{\mathrm{P}}$ (see the upper isolated limiting point in Figure 1).

We have also computed the amplitudes α_k at the first Beraha numbers B_n with $n \le 22$. For $B_2, \ldots, B_5$ the dominant amplitude vanishes as explained above. For $B_6, \ldots, B_{11}$ we find at least one vanishing amplitude, but none of them is the dominant one. Thus, none of these Beraha numbers is an isolated limiting point. Finally, for $B_{12}, \ldots, B_{22}$ all the amplitudes are nonzero. Furthermore, the product of all the amplitudes for these Beraha numbers is positive; this implies that $\det D(q) > 0$ for $q = B_{12}, \ldots, B_{22}$ because of Eq. (3.3). These results support Conjectures 7.1, 7.2, and 7.3 of [11].

3.3 $L_x = 11_{\mathrm{P}}$

The transfer matrix is 95-dimensional; it can be found in the MATHEMATICA file `transfer2.m`. We have checked that none of the amplitudes vanishes identically.

The limiting curve crosses the real axis at $q \approx 2.8900930977$. We find the following 20 approximate endpoints:

$$q \approx -0.50104 \pm 1.05084\, i \tag{3.7a}$$

$$q \approx 0.77281 \pm 2.58699\, i\,; \quad q \approx 0.77329 \pm 2.58795\, i \tag{3.7b}$$

$$q \approx 2.01541 \pm 2.39925\, i\,; \quad q \approx 2.01168 \pm 2.39892\, i \tag{3.7c}$$

$$q \approx 2.66452 \pm 1.73992\, i\,; \quad q \approx 2.67029 \pm 1.73369\, i \tag{3.7d}$$

$$q \approx 2.88992 \pm 0.35265\, i\,; \quad q \approx 2.89068 \pm 0.35252\, i \tag{3.7e}$$

$$q \approx 3.09853 \pm 0.85628\, i \tag{3.7f}$$

The endpoints (3.7b–3.7e) define eight small gaps. Finally, there is a pair of complex conjugate T-points close to $q \approx 2.902 \pm 1.015\, i$.

By inspection of Figure 3 we expect four real limiting points at the first four Beraha numbers $q = 0, 1, 2, B_5$. The first three values (i.e., $q = 0, 1, 2$) correspond to trivial isolated limiting points as all the amplitudes vanish. The fourth value $q = B_5$ has a vanishing dominant amplitude; thus, it is a true isolated limiting point. The convergence to $q = B_5$ is quite fast as shown in Table 1. The largest real zero in Table 1 converges at an approximate $1/n$ rate to the value $q_0 \approx 2.8900930977$. There are also three pairs of complex conjugate isolated limiting points: $q \approx 2.6642077467 \pm 1.2375206436\, i$, $q \approx 2.1718870063 \pm 2.0937620001\, i$, and $q \approx 0.8331263199 \pm 2.5614743076\, i$. The value of the dominant amplitude vanishes (within our numerical precision) for the first two pairs (namely, $|\alpha_\star| \sim 10^{-30}$). However, the last pair is close, but not quite equal, to the real isolated limiting point. In this case we have $|\alpha_\star| \approx 4.70 \times 10^{-3}$. We believe that there is an isolated limiting point nearby, but that the convergence to this point is still dominated by the $1/n$ rate coming from the nearby regular points in $\mathcal{B}$.

We have also checked that Conjectures 7.1, 7.2, and 7.3 of [11] hold for this strip: there is at least one vanishing amplitude for $q = B_2, \ldots, B_{12}$, while all the amplitudes are nonzero for $q = B_{13}, \ldots, B_{22}$. Only for $q = B_2, \ldots, B_5$ the dominant amplitude $\alpha_\star$ vanishes; thus, these are the only real isolated limiting points. Finally, the product $\prod_k \alpha_k > 0$ for $q = B_{13}, \ldots, B_{22}$, implying that $\det D(q) > 0$.

3.4 $L_x = 12_{\rm P}$

The transfer matrix is 232-dimensional; it can be found in the MATHEMATICA file `transfer2.m`. We have checked that none of the amplitudes vanish identically. We have not been able to compute the limiting curve $\mathcal{B}$ for this case as the transfer matrix is too large. However, we could obtain the chromatic polynomials for square-lattice strips with aspect ratios between 1 and 8 (i.e., $P_{12\times 12}$, $P_{12\times 24}$, ..., $P_{12\times 96}$). As shown in Figure 4, the zeros converge to a limiting curve very similar to the ones obtained in the previous cases. Via the direct-search method (applied to the limiting curve) we have been able to obtain an estimate of the point of the limiting curve $\mathcal{B}$ which is closest to the real axis, reading $q \approx 2.874356 \pm 0.00037\, i$.

By inspection of Figure 4 we conclude that there are four real isolated limiting points at the first four Beraha numbers. The first two of those points (i.e., $q = 0, 1$) are trivial as they correspond to the vanishing of all the amplitudes. The convergence to the other two (non-trivial) real limiting points is quite fast as can be observed from Table 1. We also find that the dominant amplitudes for $q = 2, B_5$ are very small. This evidence supports our belief that $q = 2$ and B_5 are true isolated limiting points. We also find by inspection three pairs of complex conjugate isolated limiting points: $q \approx 1.9629324150 \pm 2.2751179548\, i$, $q \approx 2.5667183607 \pm 1.4761470034\, i$, and $q \approx 2.7956875974 \pm 0.7913632912\, i$. The values of $|\alpha_\star|$ are very small for these values of q: 1.11×10^{-15}, 5.29×10^{-20}, and 1.22×10^{-16} respectively.

We have also checked that Conjectures 7.1, 7.2, and 7.3 of [11] hold for this strip: there is at least one vanishing amplitude for $q = B_2, \ldots, B_{13}$, whereas all the amplitudes are nonzero for $q = B_{14}, \ldots, B_{22}$. Furthermore, for these latter values $\prod_k \alpha_k > 0$, thus $\det D(q) > 0$ (3.3).

3.5 $L_x = 13_{\rm P}$

The transfer matrix is 498-dimensional; it can be found in the MATHEMATICA file `transfer2.m`. We have checked that none of the amplitudes vanish identically. We have not been able to compute the limiting curve $\mathcal{B}$ for this case as the transfer matrix is too large. However, we could obtain the chromatic polynomials for square-lattice strips with aspect ratios between 1 and 5 (i.e., $P_{13\times 13}$, ..., $P_{13\times 65}$). As shown in Figure 5, the zeros converge to a limiting curve very similar to the ones obtained in the previous cases. Even though the computation of the full limiting curve is too time consuming, it is very interesting to have an estimate for the value where $\mathcal{B}$ crosses the real axis. Our result is $q_0 \approx 2.9161885031$, using the direct search method.

By inspection of Figure 5 we conjecture that there are 4 real isolated limiting points corresponding to the first four Beraha numbers $q = 0, 1, 2, B_5$. The first three

are trivial zeros as all the amplitudes vanish. From Table 1 we observe that the convergence to $q = B_5$ is very fast. We have also computed the dominant amplitude for $q = B_5$. This indeed vanishes, thus $q = B_5$ is a true isolated limiting point. The largest real zero in Table 1 converges at an approximate $1/n$ rate to the value $q_0 \approx 2.9161885031$. We also find empirically three pairs of complex conjugate zeros that are likely to be isolated limiting points. As the convergence to those points is exponentially fast, the estimates obtained from the chromatic zeros for the lattice $13_{\rm P} \times 53_{\rm F}$ are expected to be close enough to the true values: $q \approx 1.7591342818 \pm 2.3988734769\,i$, $q \approx 2.4614147948 \pm 1.6813861639\,i$, and $q \approx 2.7323074066 \pm 1.0328078058\,i$. Indeed, we obtain very small dominant amplitudes for all three values of q, namely $|\alpha_\star| \approx 7.48 \times 10^{-14}$, 1.30×10^{-23}, and 1.18×10^{-21} respectively.

We have also checked that Conjectures 7.1, 7.2, and 7.3 of [11] hold for this strip: there is at least one vanishing amplitude for $q = B_2, \ldots, B_{14}$, whereas all the amplitudes are nonzero for $q = B_{15}, \ldots, B_{22}$. Furthermore, for these latter values $\prod_k \alpha_k > 0$, thus $\det D(q) > 0$ (3.3).

4 Conclusions

We have computed the transfer matrix of the zero-temperature Potts antiferromagnet defined on square-lattice strips of widths $9 \le m \le 13$ with cylindrical boundary conditions; the corresponding result with free boundary conditions are available from the authors upon request. For $m = 9, 10, 11$ we have been able to compute the limiting curves of the partition function zeros using the direct-search method. All of them have a similar qualitative shape (see Figure 6) although we observe slight differences between the limiting curves with even width and those with odd width.

In Table 2 we summarize the basic features of the limiting curves. It is worth noting that the number of connected components and endpoints increases with the strip width m. However, the gaps between those endpoints narrow as m increases. Thus, the thermodynamic limit $m \to \infty$ seems to be rather complicated in this model. This may be the cause the solution to this model is still lacking. On the other hand, the thermodynamic limit for the triangular-lattice case is smoother [33] and the model is solvable [31].

The differences between even- and odd-width strips is manifest when we try to define q_0. Only the curves corresponding to odd width cross the real axis (see Table 2). Thus, the value of q_0 can be defined for those strips. We also observe that the value of q_0 is monotonically increasing with the width m. Thus we conjecture that

Conjecture 4.1 *The limiting curves for square-lattice strips with cylindrical boundary conditions and odd width m cross the real q-axis at a point $q_0(m)$. The function $q_0(m)$ is a monotonically increasing function of m.*

Our best estimate for q_0 (assuming that Conjecture 4.1 holds) is

$$q_0(\mathrm{sq}) \gtrsim 2.9161885031\,. \tag{4.1}$$

This estimate comes from the strip with $L_x = 13_{\rm P}$. This value of q_0 is surprisingly close to the expected value for $q_c(\mathrm{sq}) = 3$ for this lattice. (It is closer to q_c than in case of the triangular lattice where $q_0(\mathrm{tri}) \approx 3.81967$ and $q_c(\mathrm{tri}) = 4$.) It might happen that for the square lattice $q_0 = q_c$. If this were the case, the limiting curve $\mathcal{B}$ when $m \to \infty$ would be qualitatively different from the triangular-lattice limiting curve computed by Baxter [31]. In particular, instead of the three domains of definition of the free energy on the positive real q-axis for the triangular-lattice case, we would have only two such domains.

In Table 2 we also observe that for even strip widths m the limiting curve does not cross the real axis. We can nevertheless define q_0 to be the closest endpoint to the real q-axis (with positive imaginary part). The real part of this quantity seems to be also a monotonically increasing function of the lattice width, while the imaginary part goes rather quickly to zero. Assuming the monotonicity of $\mathrm{Re}\, q_0$ our best estimate for q_0 would be $q_0(\mathrm{sq}) \gtrsim 2.87436$ which is smaller than (4.1). Let us now consider the quantity $\mathrm{Im}\, q_0$ and try to fit it to a power-law Ansatz. We obtain $\mathrm{Im}\, q_0 \approx 26.4 m^{-4.45}$, indicating that the true behavior might in fact be exponential. Thus, we tried an exponential Ansatz $\mathrm{Im}\, q_0 = A \times B^m$. We obtain a very good fit including all the data: $A = 0.1177(39)$ and $B = 0.6188(26)$ with $\chi^2 = 0.019$ (1 degree of freedom (DF), confidence level (level) = 89%).[6] The similarity between $B^{-1} = 1.6160(67)$ and the golden ratio $\tau = B_5^{1/2} = (1+\sqrt{5})/2 \approx 1.6180339887$ is striking. One may speculate in a possible connection between this appearance of B_5 and its role as the largest real isolated limiting point in the $m \to \infty$ limit. Thus, we state the conjecture

Conjecture 4.2 *The limiting curves for square-lattice strips with cylindrical boundary conditions and even width m do not cross the real q-axis. Let $q_0(m)$ be the closest point of the limiting curve to the real q-axis. Then, $\mathrm{Re}\, q_0(m)$ is a monotonically increasing function of m, and $\mathrm{Im}\, q_0(m) \sim B_5^{-m/2} = \tau^{-m}$ where $\tau = (1+\sqrt{5})/2$ is the golden ratio.*

Let us go back to the quantity q_0 for lattice strips with odd m. We can try to fit the data to the power-law Ansatz $A + Bm^{-\Delta}$. In all the fits we impose a lower cutoff $m \geq m_{\min}$ to the data and we study the effect of the cutoff on the estimates A, B and Δ and on the χ^2. As we increase $m_{\min}$ the estimate A decreases from 3.12688(2) down to 3.02799(5); the estimate $-B$ increases from 1.49601(4) to 2.8011(19); and the exponent Δ increases from 0.76651(40) to 1.25578(42). The χ^2 is very poor: 8.69×10^6 and 1.75×10^5 for $m_{\min} = 5$ and 7 respectively. It seems that the estimate for A tends to 3 from above. As we know that the true value for A should be bounded from above by $q_c = 3$, we can try to fit the data to the Ansatz: $3 - q_0 = Bm^{-\Delta}$. Again, we do not find any stable fit: as $m_{\min}$ increases from 5 to 11, the estimate B monotonicly goes from 2.47978(4) to 5.3807(12), and the exponent Δ grows from 1.28668(1) to 1.62265(9). Again the χ^2 is poor: it goes from 1.72×10^8 for $m_{\min} = 5$ to 5.22×10^5 for $m_{\min} = 9$.

[6] We have fitted the data shown in Table 2; the error bars are assigned to be one unit in the least significative digit.

We can play the same game with the quantity $\mathrm{Re}\, q_0$ for the lattice strips of even width m. The fits to the Ansatz $A + Bm^{-\Delta}$ are similar to the former case: as m is increased, A decreases from 3.22832(3) down to 3.02285(28); $-B$ increases from 2.95545(6) to 5.970(19); and Δ increases from 0.87657(4) to 1.4866(20). The χ^2 is poor: 5.19×10^6 and 5.30×10^3 for $m_{\min} = 4$ and 6 respectively. Again the estimate for A seems to tend to 3 from above, so we can try the next Ansatz $3 - \mathrm{Re}\, q_0 = Bm^{-\Delta}$. These fits are not very stable either: as $m_{\min}$ increases from 6 to 10, B monotonicly goes from 6.11369(19) to 8.989(12), and Δ grows from 1.54057(2) to 1.71849(54). The χ^2 is also poor: it goes from 7.02×10^5 for $m_{\min} = 6$ to 8.45×10^3 for $m_{\min} = 8$.

Our data thus suggest that, within our numerical precision, $q_0(\mathrm{sq}) = q_c(\mathrm{sq}) = 3$. We can state this finding as a conjecture

Conjecture 4.3 *For the zero-temperature square-lattice Potts antiferromagnet with cylindrical boundary conditions, $q_0 = q_c = 3$.*

The various limiting curves $\mathcal{B}$ are most similar for intermediate values of $\mathrm{Re}\, q$ (namely, $0.6 \lesssim \mathrm{Re}\, q \lesssim 2.4$). The finite-size effects are more apparent for q close to $q = 0$ and $q = q_c$. This is expected from what Baxter [31] found for the triangular lattice: the density of points around $q = 0$ and $q = q_c$ was smaller than for the other regions in the complex q-plane; thus, the convergence is expected to be slower around those two points.

In particular, we expect that eventually the rightmost branches of each limiting curve (see Figure 6) will curve back and decrease towards the expected value $q_c = 3$. Indeed, this phenomenon of "overshooting" seems to be characteristic of cylindric boundary conditions; comparison with the limiting curves $\mathcal{B}$ found in Ref. [11] for *free* boundary conditions shows that in this case the approach towards the limiting value $q_c = 3$ is monotonic. A similar remark holds true for the Potts antiferromagnet on the triangular lattice [33]. On the other hand, the leftmost endpoints of the limiting curves $\mathcal{B}$ are expected to curve back and converge to the point $q = 0$ as in the triangular-lattice case.

We have also checked Conjectures 7.1, 7.2, and 7.3 of Ref. [11, Section 7]. In particular, they state that for a square-lattice strip of width L with free or cylindrical boundary conditions,

1. At each Beraha number $q = B_2, \ldots, B_{L+1}$ there is at least one vanishing amplitude $\alpha_k(q)$;

2. For all $q = B_k$ with $k > L + 1$ none of the amplitudes $\alpha_k(q)$ vanishes; and

3. $\det D(q) > 0$ for all $q = B_k$ with $k > L + 1$.

We have shown that Conjectures 7.2 and 7.3 hold up to $k = 50$ for $L = 9_{\mathrm{P}}$, and up to $k = 22$ for $10_{\mathrm{P}} \le L \le 13_{\mathrm{P}}$. In all cases, we have found empirically that the number of vanishing amplitudes decreases from $q = B_2$ to $q = B_{L+1}$. In this latter case there is

only one vanishing amplitude and its corresponding eigenvalue is given by $\lambda = (-1)^L$. We have checked that this is so for all $L \leq 13_{\rm P}$ and $L \leq 8_{\rm F}$.[7]

Acknowledgments

We wish to thank Dario Bini for supplying us the MPSolve 2.0 package [44] and for numerous discussions about its use, and Alan Sokal for many helpful conversations throughout the course of this work. We are also grateful to a referee for suggesting the conjecture on the asymptotic behavior of $\mathrm{Im}\, q_0$. The authors' research was supported in part by CICyT (Spain) grant AEN99-0990 (J.S.).

References

[1] F.Y. Wu, Rev. Mod. Phys. **54**, 235 (1982); **55**, 315 (E) (1983).

[2] R.J. Baxter, *Exactly Solved Models in Statistical Mechanics* (Academic Press, London–New York, 1982).

[3] P. Martin, *Potts Models and Related Problems in Statistical Mechanics*. (World Scientific, Singapore, 1991).

[4] M. Aizenman and E.H. Lieb, J. Stat. Phys. **24**, 279 (1981).

[5] Y. Chow and F.Y. Wu, Phys. Rev. B **36**, 285 (1987).

[6] R.C. Read and W.T. Tutte, in *Selected Topics in Graph Theory 3*, ed. L.W. Beineke and R.J. Wilson (Academic Press, London, 1988).

[7] C. Broholm, G. Aeppli, G. Espinosa and A.S. Cooper, J. Appl. Phys. **69**, 4968 (1991).

[8] D. Huse and A.D. Rutenberg, Phys. Rev. B **45**, 7536 (1992).

[9] J. Salas and A.D. Sokal, J. Stat. Phys. **86**, 551 (1997), cond-mat/9603068.

[10] C.N. Yang and T.D. Lee, Phys. Rev. **87**, 404 (1952).

[11] J. Salas and A.D. Sokal, Transfer matrices and partition-function zeros for antiferromagnetic Potts models. I. General Theory and Square-Lattice Chromatic Polynomial, J. Stat. Phys. in press, cond-mat/0004330.

[12] A. Lenard, cited in E.H. Lieb, Phys. Rev. **162**, 162 (1967) at pp. 169–170.

[13] R.J. Baxter, J. Math. Phys. **11**, 3116 (1970).

[7] We have only found one exception to this empirical behavior: for $L = 5_{\rm F}$ there are two eigenvalues $\lambda = -1$.

[14] R.J. Baxter, Proc. Roy. Soc. London A **383**, 43 (1982).

[15] M. den Nijs, M.P. Nightingale and M. Schick, Phys. Rev. B **26**, 2490 (1982).

[16] J.K. Burton Jr. and C.L. Henley, J. Phys. A **30**, 8385 (1997), cond-mat/9708171.

[17] J. Salas and A.D. Sokal, J. Stat. Phys. **92**, 729 (1998), cond-mat/9801079.

[18] S.L.A. de Queiroz, T. Paiva, J.S. de Sá Martins and R.R. dos Santos, Phys. Rev. E **59**, 2772 (1999), cond-mat/9812341.

[19] S.J. Ferreira and A.D. Sokal, J. Stat. Phys. **96**, 461 (1999), cond-mat/9811345.

[20] S. Beraha, J. Kahane and N.J. Weiss, Proc. Nat. Acad. Sci. USA **72**, 4209 (1975).

[21] S. Beraha, J. Kahane and N.J. Weiss, in *Studies in Foundations and Combinatorics* (Advances in Mathematics Supplementary Studies, Vol. 1), ed. G.-C. Rota (Academic Press, New York, 1978).

[22] M. Roček, R. Shrock and S.-H. Tsai, Physica A **252**, 505 (1998), cond-mat/9712148.

[23] M. Roček, R. Shrock and S.-H. Tsai, Physica A **259**, 367 (1998), cond-mat/9807106.

[24] S.-C. Chang and R. Shrock, Physica A **290**, 402 (2001), cond-mat/0004161.

[25] R. Shrock and S.-H. Tsai, Phys. Rev. E **55**, 5165 (1997), cond-mat/9612249.

[26] R. Shrock and S.-H. Tsai, Phys. Rev. E **60**, 3512 (1999), cond-mat/9910377.

[27] N. Biggs, The chromatic polynomial of the $3 \times n$ toroidal lattice, London School of Economics CDAM Research Report LSE-CDAM-99-05 (1999).

[28] N. Biggs and R. Shrock, J. Phys. A **32**, L489 (1999), cond-mat/0001407.

[29] R. Shrock and S.-H. Tsai, Physica A **275**, 429 (2000), cond-mat/9907403.

[30] S.-C. Chang and R. Shrock, $T = 0$ partition functions for Potts antiferromagnet on lattice strips with fully periodic boundary conditions, cond-mat/0007491.

[31] R.J. Baxter, J. Phys. A **20**, 5241 (1987).

[32] R. Shrock and S.-H. Tsai, Phys. Rev. E **56**, 1342 (1997), cond-mat/9703249.

[33] J.L. Jacobsen, J. Salas and A.D. Sokal, Transfer matrices and partition-function zeros for antiferromagnetic Potts models. III. Triangular-Lattice Chromatic Polynomial, in preparation.

[34] R. Shrock, Chromatic Polynomials and their Zeros and Asymptotic Limits for Families of Graphs, in the *Proceedings of the 1999 British Combinatorial Conference BCC99* (July, 1999), Disc. Math. in press, cond-mat/9908387.

[35] J.L. Jacobsen, J. Salas and A.D. Sokal, Transfer matrices and partition-function zeros for antiferromagnetic Potts models. IV. Periodic boundary conditions in the longitudinal direction, in preparation.

[36] S. Beraha, unpublished, circa 1974.

[37] P.W. Kasteleyn and C.M. Fortuin, J. Phys. Soc. Japan **26** (Suppl.), 11 (1969).

[38] C.M. Fortuin and P.W. Kasteleyn, Physica **57**, 536 (1972).

[39] R.P. Stanley, *Enumerative Combinatorics*, vol. 1 (Wadsworth & Brooks/Cole, Monterey, CA, 1986). Reprinted by Cambridge University Press, 1999.

[40] H.W.J. Blöte and M.P. Nightingale, Physica **112A**, 405 (1982).

[41] J.L. Jacobsen and J. Cardy, Nucl. Phys. B **515**[FS], 701 (1998), cond-mat/9711279.

[42] N.L. Biggs, R.M. Damerell and D.A. Sands, J. Combin. Theory B **12** (1972) 123.

[43] S. Beraha, J. Kahane and N.J. Weiss, J. Combin. Theory B **28**, 52 (1980).

[44] D.A. Bini and G. Fiorentino, Numerical computation of polynomial roots: MPSolve – Version 2.0. FRISCO report (1998). Available at `http://www.dm.unipi.it/pages/bini/public_html/papers/mpsolve.ps.Z`. Software package available at `http://www.dm.unipi.it/pages/bini/public_html/software/mps2.tar.gz`.

Lattice	3rd Zero	4th Zero	5th Zero
$9_P \times 9_F$	2	2.620608391171	2.660519126718
$9_P \times 18_F$	2	2.618033988527	
$9_P \times 27_F$	2	2.618033988750	2.791347005408
$9_P \times 36_F$	2	2.618033988750	
$9_P \times 45_F$	2	2.618033988750	2.814819876147
$9_P \times 54_F$	2	2.618033988750	
$9_P \times 63_F$	2	2.618033988750	2.824928798467
$9_P \times 72_F$	2	2.618033988750	
$9_P \times 81_F$	2	2.618033988750	2.830572841537
$9_P \times 90_F$	2	2.618033988750	
$10_P \times 10_F$	2.000000000000	2.614232442467	
$10_P \times 20_F$	2.000000000000	2.618033987905	
$10_P \times 30_F$	2.000000000000	2.618033988750	
$10_P \times 40_F$	2.000000000000	2.618033988750	
$10_P \times 50_F$	2.000000000000	2.618033988750	
$10_P \times 60_F$	2.000000000000	2.618033988750	
$10_P \times 70_F$	2.000000000000	2.618033988750	
$10_P \times 80_F$	2.000000000000	2.618033988750	
$10_P \times 90_F$	2.000000000000	2.618033988750	
$10_P \times 100_F$	2.000000000000	2.618033988750	
$11_P \times 11_F$	2	2.618035720465	2.731088786113
$11_P \times 22_F$	2	2.618033988750	
$11_P \times 33_F$	2	2.618033988750	2.836691210598
$11_P \times 44_F$	2	2.618033988750	
$11_P \times 55_F$	2	2.618033988750	2.857656644942
$11_P \times 66_F$	2	2.618033988750	
$11_P \times 77_F$	2	2.618033988750	2.866767905070
$11_P \times 88_F$	2	2.618033988750	
$11_P \times 99_F$	2	2.618033988750	2.871875414535
$11_P \times 110_F$	2	2.618033988750	
$12_P \times 12_F$	2.000000000000	2.618032077436	
$12_P \times 24_F$	2.000000000000	2.618033988750	
$12_P \times 36_F$	2.000000000000	2.618033988750	
$12_P \times 48_F$	2.000000000000	2.618033988750	
$12_P \times 60_F$	2.000000000000	2.618033988750	
$12_P \times 72_F$	2.000000000000	2.618033988750	
$12_P \times 84_F$	2.000000000000	2.618033988750	
$12_P \times 96_F$	2.000000000000	2.618033988750	
$13_P \times 13_F$	2	2.618033988926	2.775231591227
$13_P \times 26_F$	2	2.618033988750	
$13_P \times 39_F$	2	2.618033988750	2.867878041004
$13_P \times 52_F$	2	2.618033988750	
$13_P \times 65_F$	2	2.618033988750	2.886773116380
Beraha	2	2.618033988750	

Table 1: Real zeros of the chromatic polynomials of finite square-lattice strips with periodic boundary conditions in the transverse direction and free boundary conditions in the longitudinal direction, to 12 decimal places. A blank means that the zero in question is absent. The first two real zeros $q = 0, 1$ are exact on all lattices; the third real zero $q = 2$ is exact on all lattices of odd width. "Beraha" indicates the Beraha numbers $B_4 = 2$ and $B_5 = (3 + \sqrt{5})/2$.

	Eigenvalue-Crossing Curves $\mathcal{B}$								Isolated Points	
Lattice	# C	# E	# T	# D	# ER	$\min \operatorname{Re} q$	q_0	$\max \operatorname{Re} q$	# RI	# CI
3_P	0	0	0	0	0				3	0
4_P	3	8	0	1	0	0.709803	$[2.253370, 2.351688]$	2.995331	3	0
5_P	5	10	0	0	0	0.165021	2.691684	2.691684	4	0
6_P	3	10	2	1	0	−0.131889	$[2.608943, 2.613228]$	3.171192	3	1
7_P	7	16	2	0	0	−0.296250	2.788378	2.839016	4	1
8_P	6	16	4	0	0	−0.390864	$2.751531 \pm 0.002531\, i^*$	3.211132	4	2
9_P	9	20	2	0	0	−0.446992	2.850572	3.011232	4	4
10_P	$10^\dagger$	$22^\dagger$	$2^\dagger$	$0^\dagger$	$0^\dagger$	−0.48079	$2.82813 \pm 0.00097\, i^*$.	3.21691	4	$6^\dagger$
11_P	$9^\dagger$	$20^\dagger$	$2^\dagger$	$0^\dagger$	$0^\dagger$	−0.50104	2.890093	3.09853	4	$6^\dagger$
12_P							$2.87436 \pm 0.00037\, i^*$		4	$6^\dagger$
13_P							2.916189		4	$6^\dagger$

Table 2: Summary of qualitative results for the eigenvalue-crossing curves $\mathcal{B}$ and for the isolated limiting points of zeros. For each square-lattice strip considered in this paper, we give the number of connected components of $\mathcal{B}$ (# C), the number of endpoints (# E), the number of T points (# T), the number of double points (# D), and the number of enclosed regions (# ER); we give the minimum value of $\operatorname{Re} q$ on $\mathcal{B}$, the value(s) q_0 where $\mathcal{B}$ intersects the real axis (* denotes an almost-crossing), and the maximum value of $\operatorname{Re} q$ on $\mathcal{B}$. We also report the number of real isolated limiting points of zeros (# RI) [which are always successive Beraha numbers B_2, B_3, ...] and the number of complex conjugate pairs of isolated limiting points (# CI). The symbol † indicates uncertain results. The results for $L \le 8_P$ are included for comparison; they are taken from Ref. [11].

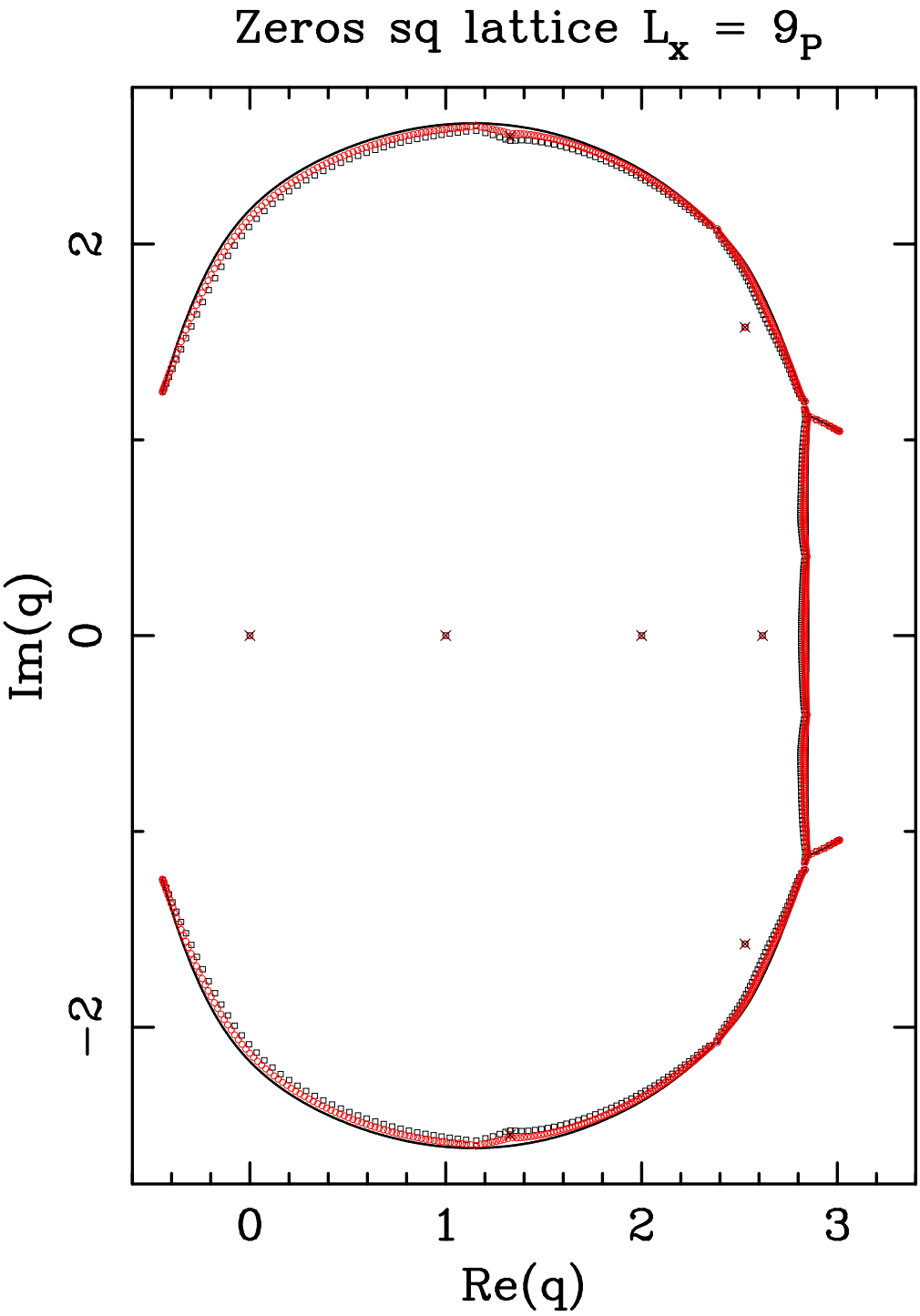

Figure 1: Zeros of the partition function of the q-state Potts antiferromagnet on the square lattices $9_P \times 45_F$ (squares), $9_P \times 90_F$ (circles) and $9_P \times \infty_F$ (solid line). The isolated limiting zeros are depicted by a $\times$. The limiting curve was computed using the direct-search method, except the endpoints that were computed using the resultant method.

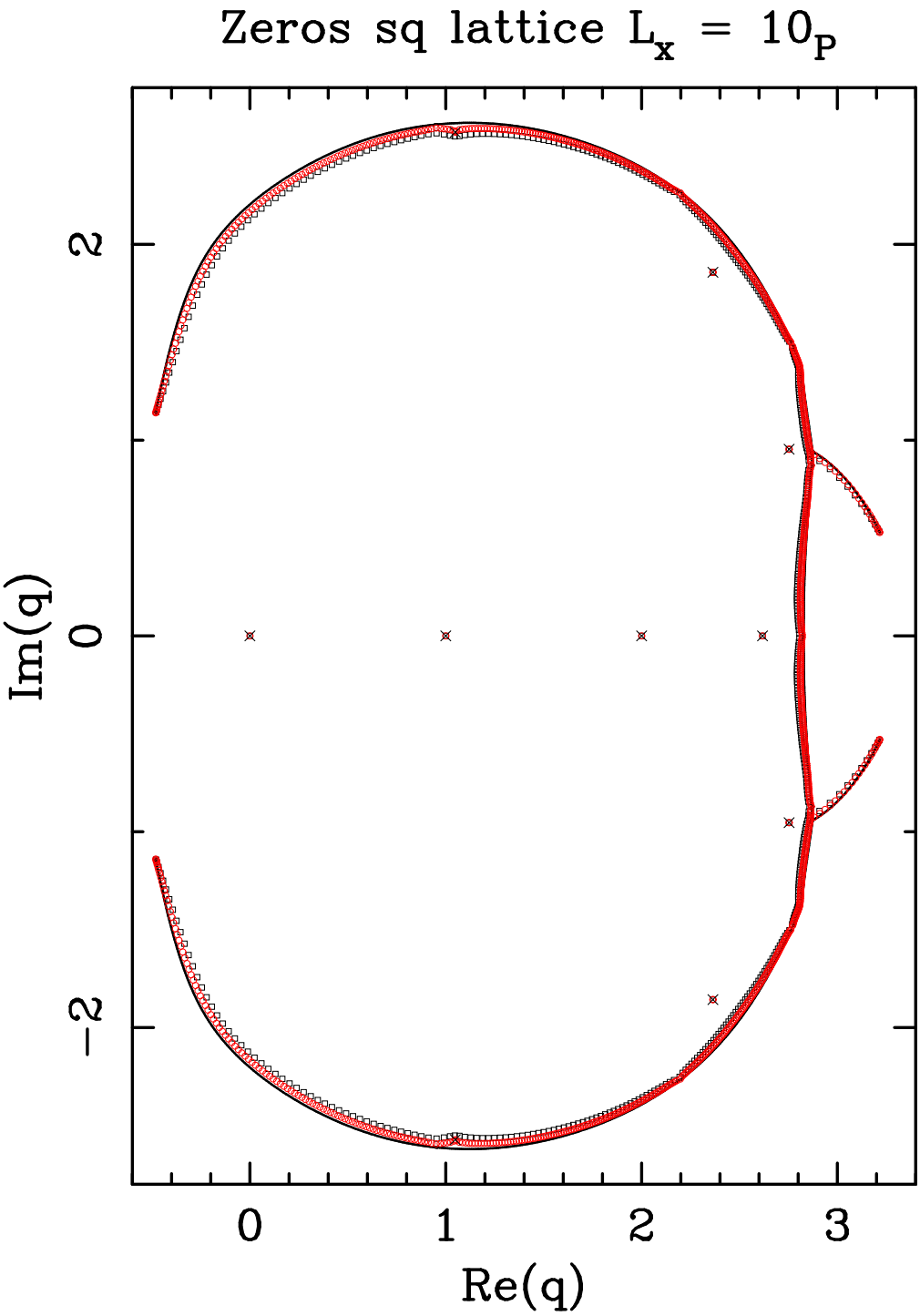

Figure 2: Zeros of the partition function of the q-state Potts antiferromagnet on the square lattices $10_P \times 50_F$ (squares), $10_P \times 100_F$ (circles) and $10_P \times \infty_F$ (solid line). The isolated limiting zeros are depicted by a $\times$. The limiting curve was computed using the direct-search method.

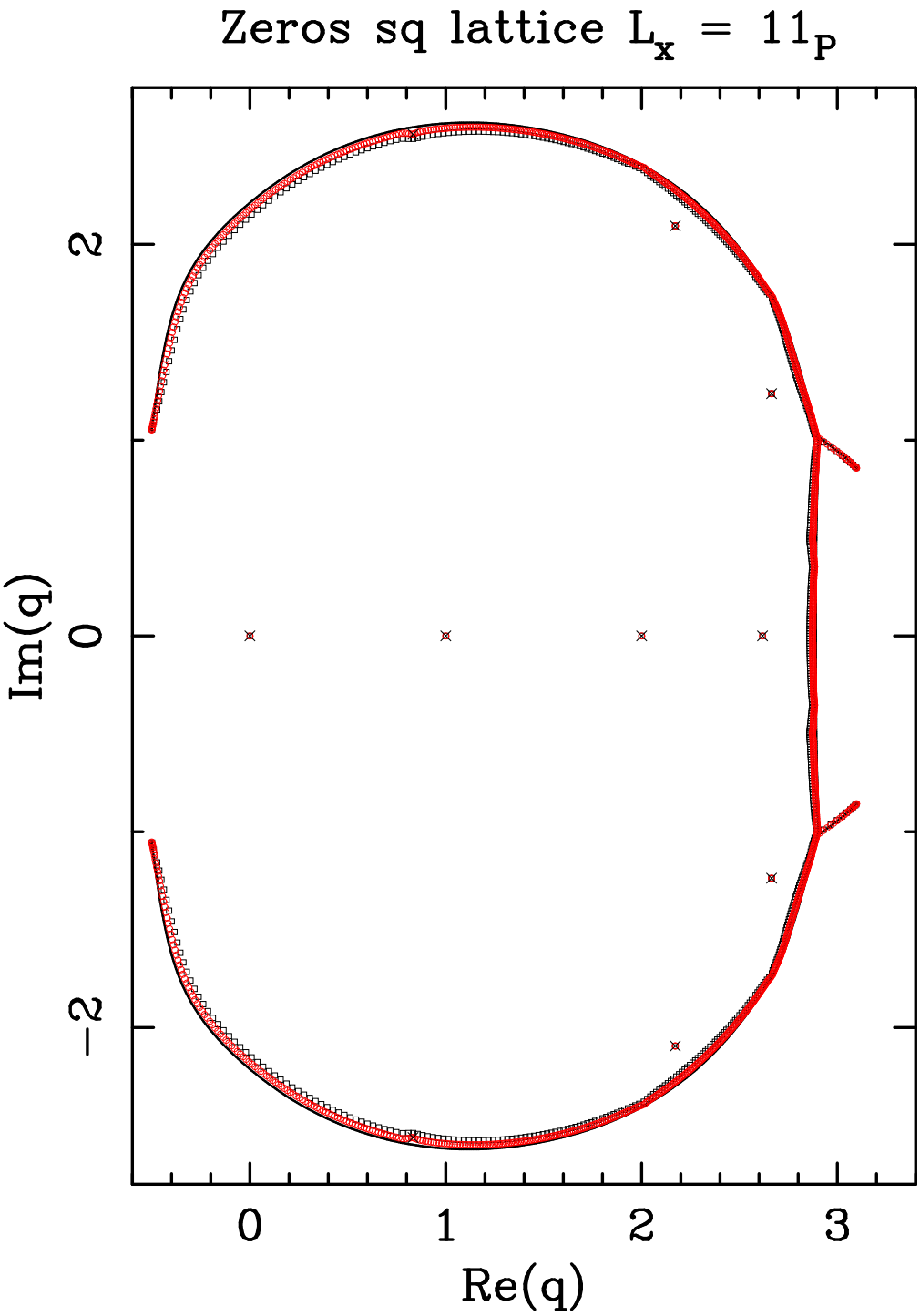

Figure 3: Zeros of the partition function of the q-state Potts antiferromagnet on the square lattices $11_P \times 55_F$ (squares), $11_P \times 110_F$ (circles) and $11_P \times \infty_F$ (solid line). The isolated limiting zeros are depicted by a $\times$. The limiting curve was computed using the direct-search method.

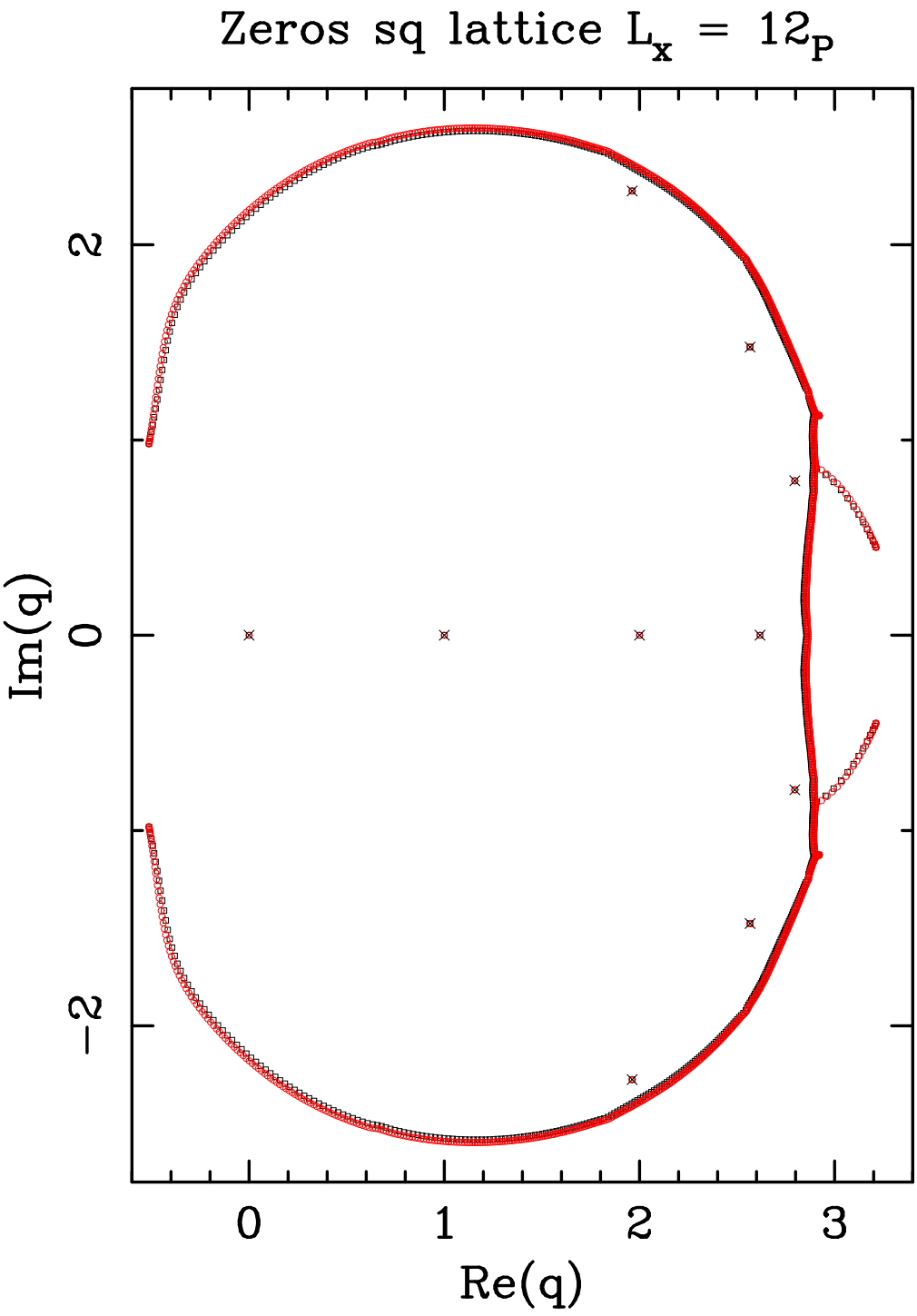

Figure 4: Zeros of the partition function of the q-state Potts antiferromagnet on the square lattices $12_P \times 60_F$ (squares) and $12_P \times 96_F$ (circles). The isolated limiting zeros are depicted by a $\times$.

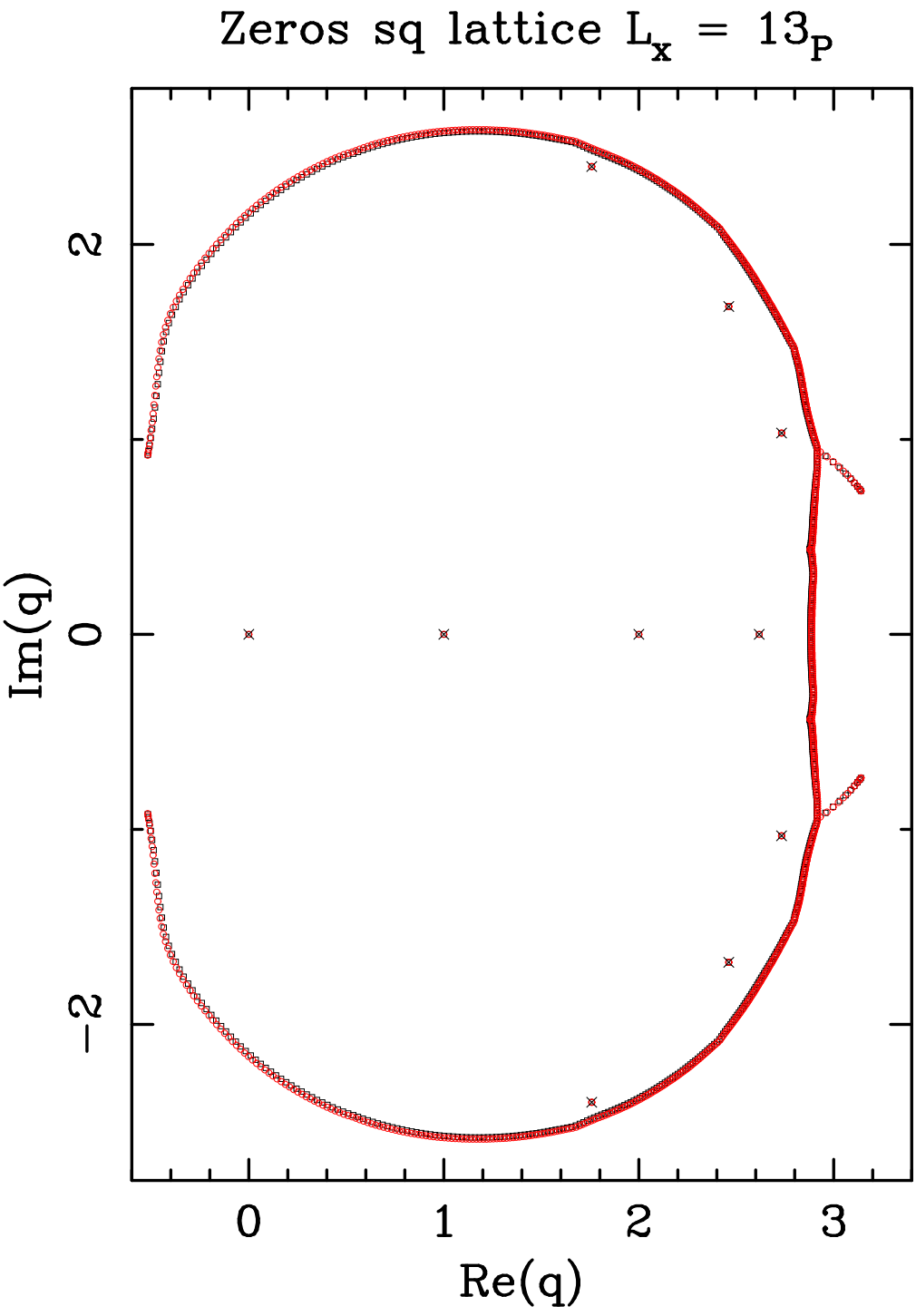

Figure 5: Zeros of the partition function of the q-state Potts antiferromagnet on the square lattices $13_P \times 52_F$ (squares) and $13_P \times 65_F$ (circles). The isolated limiting zeros are depicted by a $\times$.

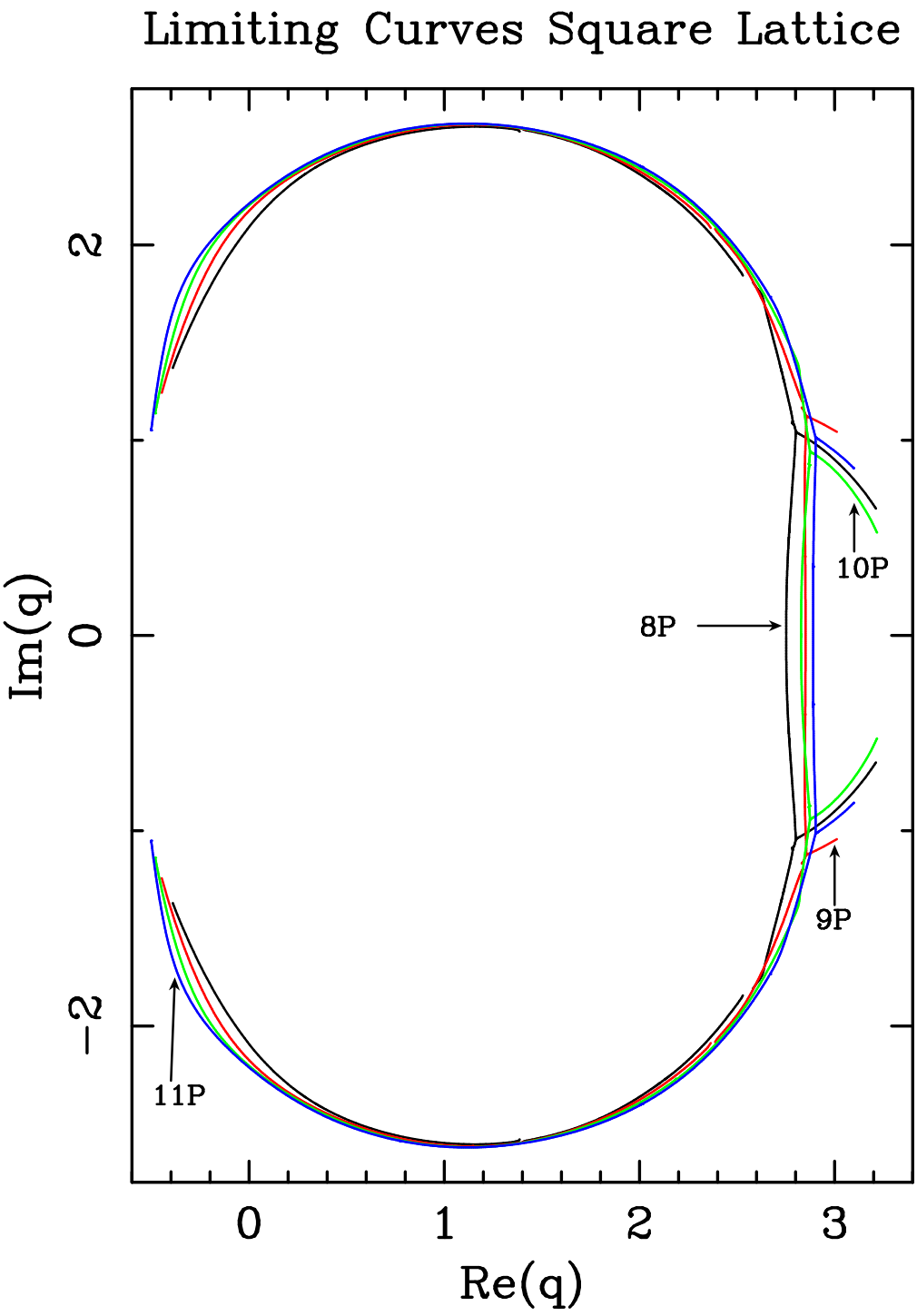

Figure 6: Limiting curves for the square-lattice strips $L_{\rm P} \times \infty_{\rm F}$ with $8 \le L \le 11$. The curve for $L = 8$ was obtained in [11].